Colloid Polym Sci (2009) 287:1155–1165
DOI 10.1007/s00396-009-2075-3

ORIGINAL CONTRIBUTION

# Dissipative crystallization of aqueous solution of sodium polymethacrylate

**Tsuneo Okubo · Akira Hagiwara · Hiromi Kitano · Junichi Okamoto · Shinya Takahashi · Akira Tsuchida**

Received: 8 June 2009 / Accepted: 24 June 2009 / Published online: 11 July 2009


**Abstract** Drying dissipative structures of aqueous solution of sodium polymethacrylate (NaPMA) were studied on a cover glass, a watch glass, and a glass dish. Any convectional and sedimentation patterns did not appear during the course of dryness. Several important findings on the drying patterns are reported. Firstly, spherulite and hedrite dissipative crystals were observed when the polymer solutions were dried. The crystalline structures changed from hedrites to spherulites as polymer concentration increased. Secondary, the coupled structures of the spherulites and the broad rings were observed for NaPMA at the outside edge of the broad ring. However, the coupled crystalline structures of the lamellaes from the broad ring and the spherulites, which were observed for poly(ethylene glycol) (Okubo et al. 2009), were not observed clearly for NaPMA system. Thirdly, size of the broad ring at the outside edge of the dried film increased sharply as polymer concentration increased.

**Keywords** Sodium polymethacrylate · Dissipative crystallization · Dissipative structure · Drying pattern · Spherulite · Hedrite

T. Okubo (✉)
Institute for Colloidal Organization,
Hatoyama 3-1-112,
Uji, Kyoto 611-0012, Japan
e-mail: okubotsu@ybb.ne.jp

T. Okubo
Graduate School of Science and Technology,
Yamagata University,
Johnan 4-3-16,
Yonezawa, Yamagata 992-8510, Japan

A. Hagiwara · H. Kitano
Department of Applied Chemistry, University of Toyama,
Toyama 930-8555, Japan

J. Okamoto · S. Takahashi · A. Tsuchida
Department of Applied Chemistry, Gifu University,
Yanagido 1,
Gifu 501-1193, Japan

## Introduction

Most structural patterns in nature form via self-organization accompanied with the dissipation of free energy and in the non-equilibrium state. In order to know the mechanisms of the dissipative self-organization of the simple model systems instead of the much complex nature itself, the authors have studied the convectional, sedimentation, and drying dissipative patterns during the course of drying colloidal suspensions and solutions as systematically as possible, though the three kinds of patterns are correlated strongly and overlapped with each other [1, 2].

Most famous convectional pattern is the hexagonal circulating one, Benard cell and has been observed when liquids contain plate-like colloidal particles as monitors and are heated homogeneously in a plain pan [3–5]. Another typical convectional pattern is the Terada cell, where the spoke-like lines prevail in the whole area at the liquid surface and accompanied with the huge number of small cell convections in the normal direction of the spoke lines [6–9]. The distorted Benard and Terada cells were observed with the naked eyes in the initial course of dryness of the Chinese black ink in a glass dish [10], 100% ethanol suspensions of colloidal silica spheres [11], a cup of Miso-soup [12], coffee [13], black tea [14], and colloidal crystals of poly(methyl methacrylate; PMMA) spheres on a cover glass and a watch glass [15, 16].

The whole growing processes of the convectional patterns are summarized as seven steps [10–16]. Firstly, at the initial stage of convection, appearance, and disappearance of the circulating lines (irregular circulations) takes place at random in their direction accompanied with the gravitational upward transportation of heat. Secondary, global flow of the convection takes place at the surface layers from the center toward outward edge of the liquid. Thirdly, the cooperated distorted Benard cells form at the liquid surface. Fourthly, the reversed inward global flow of convection is observed at the liquid surface, which is mainly due to the Marangoni convection. Fifthly, growing of the spoke lines from the outside edge to the central area takes place at the liquid surface layers. Sixthly, the clusters and further bundles of the spoke lines are formed at the final stage of convection. Growing of the broad ring-like sedimentation and drying patterns are formed in the middle and/or final stage of convections. The bundles at the final stage of convection are considered also to be the sedimentation ones, and are further transformed to the drying patterns with fine structures.

Sedimentation dissipative patterns have been studied in detail in the course of drying suspensions of colloidal silica spheres (183 nm to 1.2 μm in diameter) [17–22], size-fractionated bentonite particles [23], green tea (Ocha) [24] and Miso-soup [12], for the first time, in our laboratory. The broad ring patterns were formed within several 10 min in suspension state by the convectional flow of water and the colloidal particles. It was clarified that the sedimentary particles were suspended above the substrate by the electrical double layers and always moved by the balancing of the external force fields including convectional flow and sedimentation. Furthermore, the sharpness of the sedimentation broad rings was sensitive to the change in the room temperature and/or humidity [17]. Quite recently, it was clarified that the dynamic bundle-like sedimentation patterns formed cooperatively from the spoke line-like convectional structures of colloidal particles for coffee [13], black tea [14], and colloidal crystals of PMMA spheres [15, 16].

Drying dissipative patterns have been studied for suspensions and solutions of colloidal particles [1, 2, 10–13, 17–30], linear-type synthetic and bio-polyelectrolytes [31, 32], water-soluble neutral polymers [33, 34], ionic and non-ionic detergents [35–37], gels [38], and dyes [39] mainly on a cover glass. The macroscopic broad ring patterns of the hill accumulated with the solutes in the outside edges formed on a cover glass, a watch glass, and a glass dish. The broad rings moved inward when solute concentration decreased and/or solute size increased. For the non-spherical particles, the round hill was formed in the center area in addition to the broad ring [23]. Macroscopic spoke-like cracks or fine hills including flickering spoke-like ones were also observed for many solutes. Furthermore, beautiful microscopic fractal patterns such as earth worm-like, branch-like, arc-like, block-like, star-like, cross-like, and string-like ones were observed. These microscopic drying patterns were often reflected from the shape, size, and/or flexibility of the solutes themselves. Microscopic patterns also formed by the translational Brownian diffusion of the solutes and the electrostatic and/or the hydrophobic interactions between solutes and/or between the solutes and the substrate in the course of the solidification. One of the very important findings in our experiments is that the primitive vague sedimentation patterns were formed already in the liquid phase before dryness and they grew toward fine structures in the processes of solidification [23].

Deegan et al. [40, 41] have reported the traces of spoke-like patterns in the suspensions of polystyrene spheres (1 μm in diameter) under a microscope. They introduced the capillary flow theory accompanied with the pinning effect of the contact line of the drying drop. From our series of drying experiments for suspensions and solutions, however, the important role of the pinning effect was not always supported except experiments at high particle concentrations and/or for small colloidal particles. In general, the broad ring-like drying patterns are always formed irrespective of the solutes and substrates used. However, they moved toward central area and their size became small until the solute–solute repulsive or attractive interactions are strong enough to form the inter-solute structures on substrates such as critical concentration of the structure formation of colloidal crystals [15, 16], bio-polymer's helix, and sheet structures [31] or detergent's micelles [35, 36]. Calchile et al. [42, 43] reported that the droplets of completely wetting liquids deposited on a thoroughly smooth and wetting surface for which no contact line anchoring occurs. The author believes that the convectional flow of solvent and solutes is essentially important throughout the convectional, sedimentation, and drying pattern formation. The pinning effect was not supported also in a glass dish, where drying frontier starts from the central area of a vessel substrate and developed toward outside. It should be mentioned that theoretical studies for the convectional patterns have been made hitherto, but these are not always successful yet [40, 41, 44–51]. It should be further noted that information on the size, shape, conformation, and/or flexibility of particles and polymers, for example, is transformed cooperatively and further accompanied with the amplification and selection processes toward the succeeding sedimentation and drying patterns during the course of dryness of solutions and suspensions [32, 35–37].

Recently, drying dissipative patterns of poly(ethylene glycol) (PEG, which is also named as poly(ethylene oxide) or poly(oxyethylene)) having molecular weights from 200

to 3,500,000 have been studied on the macroscopic and microscopic scales [52]. The dissipative crystalline structures of hedrite and spherulite were observed on a cover glass, a watch glass, and a glass dish. Lamellaes were formed along the ring patterns especially at high concentrations and high molecular weights. The coupled patterns of the spherulites and the lamellaes were formed especially in a watch glass. In this work, dissipative crystalline structures such as hedrites and spherulites were also observed in the dried film of sodium polymethacrylate (NaPMA), for the first time, in our laboratory. NaPMA is one of the typical anionic and hydrophobic polyelectrolytes. One of the main purposes of this work is the clarification of the importance of the convectional flow on the drying crystalline structural formation in the drying patterns and the mechanisms of the dissipative crystallization during the course of dryness of NaPMA.

## Experimental

### Materials

Sodium polymethacrylate was synthesized for 24 h at 60 °C from the mixtures of α, α'-azobisisobutyronitrile (58.2 mg), methanol (35.4 ml), 2-mercaptoethanol (0.125 ml), and methacrylic acid (3.0 ml). The mixture was purged with nitrogen gas for 30 min before polymerization treatment. The product, poly(methacrylic acid) (HPMA) was dialyzed with the membrane film (3,500 of molecular weight cut-off, Spectra/Por®, regenerated cellulose, Spectrum Laboratories, Inc., Rancho Dominguez, CA, USA). Then NaPMA was obtained by the neutralization of the part of HPMA with the equivalent amount of the aqueous solution of sodium hydroxide. Number average ($M_n$) and weight average molecular weights ($M_w$) of HPMA and NaPMA measured on a Gel-Permeation-Chromatography (Shimadzu LC-10 AD pump, Kyoto and Waters R401 Differential refractometer) were 9,520 and 12,900 and 9,760 and 14,200, respectively. The ratios $M_w/M_n$ were 1.35 and 1.45 for HPMA and NaPMA, respectively. The column used was Wakobeads G-30 (Wako Chemicals Co., Osaka) and the standard samples were Pullulan from Showa Denko Co. Mobile phase was 0.1 M aqueous phosphate buffer (pH 6.8). Flow rate was 0.4 ml/min. Tacticity of the HPMA was discussed by $^1$H-NMR measurements. The triad compositions of rr (syndiotactic), mr (heterotactic), and mm (isotactic) were evaluated as 64:31:5, which supports the fact that HPMA obtained in this work is mainly atactic, but containing a small amount of syndiotactic configuration. The water used for the sample preparation was purified by a Milli-Q reagent grade system (Milli-RO5 plus and Milli-Q plus, Millipore, Bedford, MA, USA).

### Observation of the dissipative structures

Aliquot, 0.1 ml, of the aqueous solution of NaPMA sample was carefully and gently placed onto a micro cover glass (30×30 mm, No. 1, thickness 0.12 to 0.17 mm, Matsunami Glass, Kishiwada, Osaka) set in a plastic dish (type NH-52, 52 mm in diameter, 8 mm in depth, As One Co., Tokyo). The cover glass was used without further rinse. Four milliliters of the solution was set on a medium watch glass (70 mm, TOP Co. Tokyo). Five milliliters of the solution was put into a medium glass dish (42 mm in inner diameter and 15 mm in height, code 305-02, TOP Co.). The disposable serological pipets (1 ml and 10 ml, Corning Lab. Sci., Co.) were used for the putting the suspension in the substrates. The patterns during the course of dryness were observed for the solutions on a desk covered with a black plastic sheet. The room temperature was regulated at 24 °C. Humidity of the room was not regulated and between 47% and 58%.

Macroscopic patterns were observed on a Canon EOS 10 D digital camera with a macro-lens (EF 50 mm, $f$=2.5) plus a life-size converter EF or a zoom-lens (Canon, EF28-70 mm, 1:2.8) on a cover glass and a medium glass dish or a medium watch glass, respectively. Microscopic drying patterns were observed with a metallurgical microscope (PME-3, Olympus Co., Tokyo). Thickness profiles of the dried films on a cover glass were measured on a laser 3D profile microscope (type VK-8500, Keyence Co., Osaka, Japan). Polarizing microscopic pictures were taken on a Shimadzu polarizing microscope (type Kalnew 53255, Shimadzu, Kyoto) with a CCD camera (type TNC4604J, Kenis Ltd, Osaka).

## Results and discussion

### Macroscopic and microscopic drying patterns of NaPMA solutions on a cover glass

Figure 1 shows the typical macroscopic drying patterns of NaPMA solutions at the concentrations from 0.006 monoM (a) to 0.02 monoM (e). Frame size of these pictures is 14×14 mm. The broad ring patterns were always recognized irrespective of the initial polymer concentrations. Sizes of the broad rings are shown in Fig. 2 as a function of polymer concentration. The sizes on a watch glass and a glass dish are also plotted in the figure. The ratios of the final size of the broad rings in diameter ($d_f$) against the initial size of the liquid in diameter ($d_i$) on a cover glass shown by open circles increased as the initial polymer concentration increased. Here, the size of the broad rings was measured as the distance between the outside edges, not the thickness peak positions of the broad rings. Increase in the broad ring

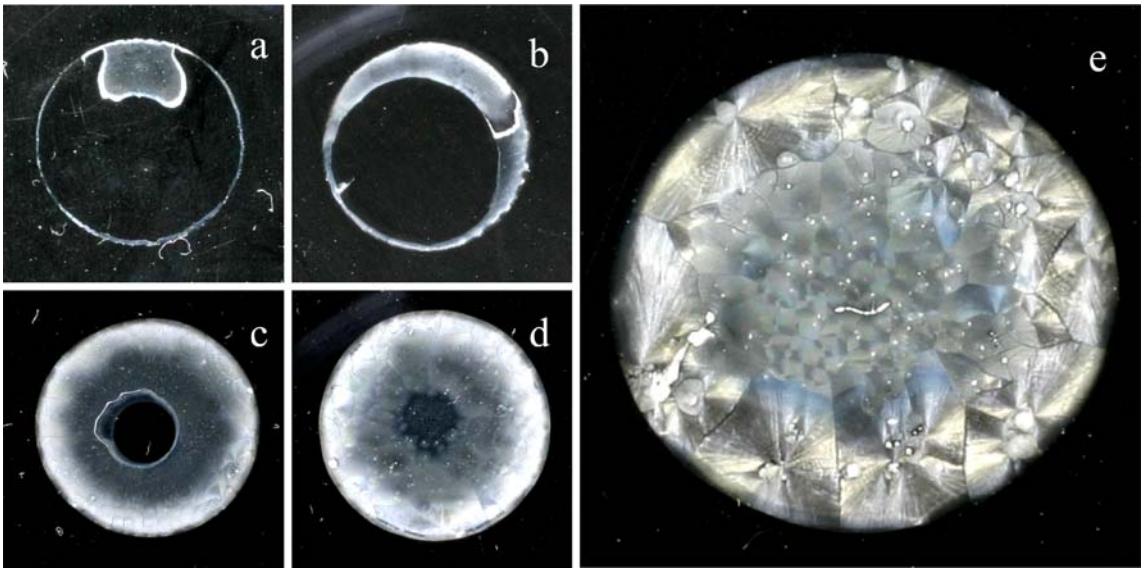


**Fig. 1** Drying dissipative patterns of aqueous NaPMA solution on a cover glass at 24 °C; 0.1 ml, **a** [NaPMA]=0.0006 monoM, after 4 h 50 m, **b** 0.002 monoM, **c** 0.006 monoM, **d** 0.01 monoM, and **e** 0.02 monoM, after 7 h 55 m; frame size of the pictures is 14×14 mm

size with the concentration is due to the fact that the inter-polymer crystalline structure is formed within the small areas when the polymer concentration is low. As is described already in "Introduction" section, the broad ring size decreases until the solute–solute repulsions or attractions are strong enough to form the inter-solute structures such as colloidal crystals [15, 16], helix or sheet structures [31], and detergent's micelles [35, 36]. It should be recalled that the change in the size of broad rings does not support the pinning effect of the contact line proposed by Deegan et al. [40, 41].

Figure 1 clearly shows the appearance of the crystalline structures, and their size increased as the initial polymer concentration increased. Figure 1e demonstrates that the single crystals are spherulite from the authors' experience on the dissipative crystalline patterns of poly(ethylene glycol) [52]. The size of the single crystals is especially large in the areas of the broad rings, where the dried film is

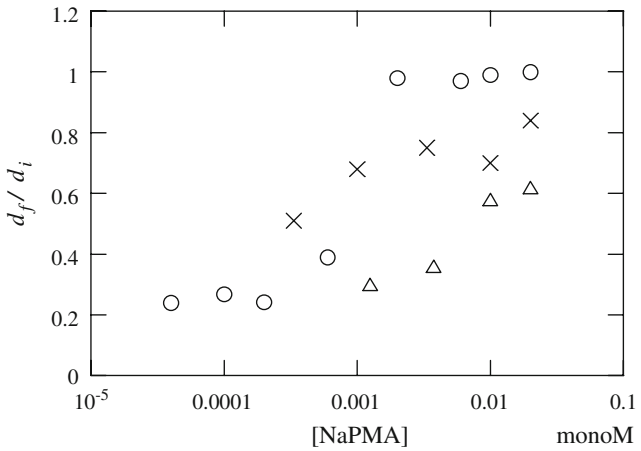


**Fig. 2** Plots of $d_f/d_i$ of NaPMA as a function of polymer concentration on a cover glass (*open circles*), a watch glass (*crosses*), and a glass dish (*open triangles*)

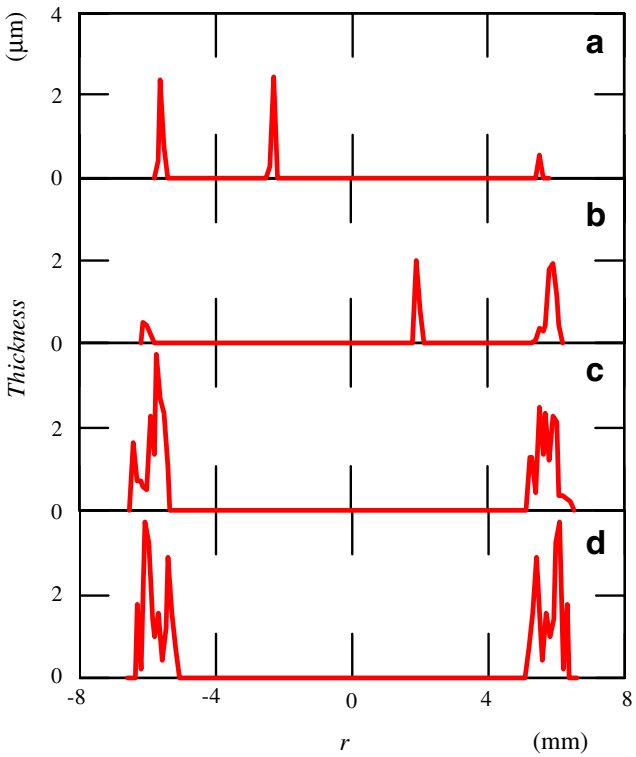


**Fig. 3** Thickness profiles of the dried film of NaPMA solution on a cover glass as a function of the distances from the center at 24 °C. **a** [NaPMA]=0.0006 monoM, **b** 0.006 monoM, **c** 0.01 monoM, and **d** 0.02 monoM

thick and the polymer accumulation is substantial compared with other areas. As is clear in Fig. 1(a to e), the spherulites were packed densely and arrayed along the broad ring. Furthermore, most of the spherulites were cut sharply by the outside broad ring lines (see Fig. 1e, for example). This supports that the strong coupling of the broad ring formation and the spherulite crystallization. Crystallization on a cover glass must be influenced significantly by the shearing forces induced by the convectional flow of the liquid during the course of dryness. It should be mentioned here that the macroscopic drying patterns of NaPMA at the initial concentrations at $4\times10^{-5}$ monoM and $1\times10^{-4}$ monoM showed only the traces of the fine ring. The drying pattern at $2\times10^{-4}$ monoM was quite similar to that at $6\times10^{-4}$ monoM shown in Fig. 1a. Drying times were around 4 h and increased slightly as the initial polymer concentration decreased.

Figure 3 shows the thickness profiles of the dried films as a function of the distance from the film center ($r$) at 0.0006 monoM (a) to 0.02 monoM (d). The profiles demonstrate the formation of the broad ring patterns at the outside edge clearly, and their size increased slightly as polymer concentration increased. It should be mentioned here that the sharp peaks exist in between the two peaks corresponding the outside edges in the pictures a and b. These peaks are from the broad rings of the localized small dried areas as is shown in Fig. 1a (upper area), for example. Furthermore, the peaks of the broad rings in c and d were very rough, which is clearly due to the formation of the sharp shaped spherulite crystals at the broad ring area.

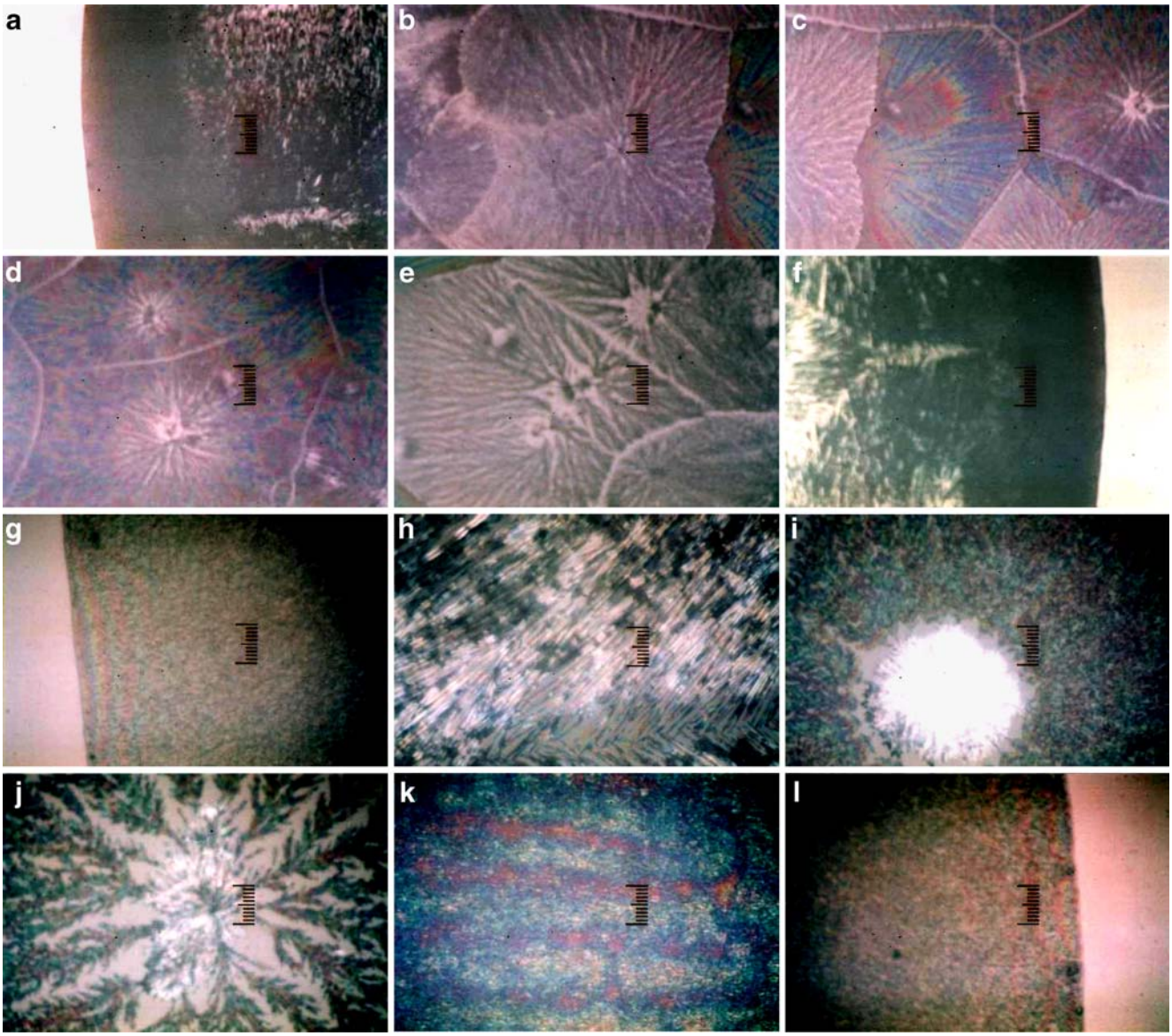


**Fig. 4** Microscopic drying dissipative patterns of aqueous NaPMA solution on a cover glass at 24 °C. Code 1044, [NaPMA]=0.02 monoM, **a** to **f** and **g** to **l** are the pictures from the left edge to the right, full scales are 200 μm (**a** to **f**) and 25 μm (**g** to **l**), respectively

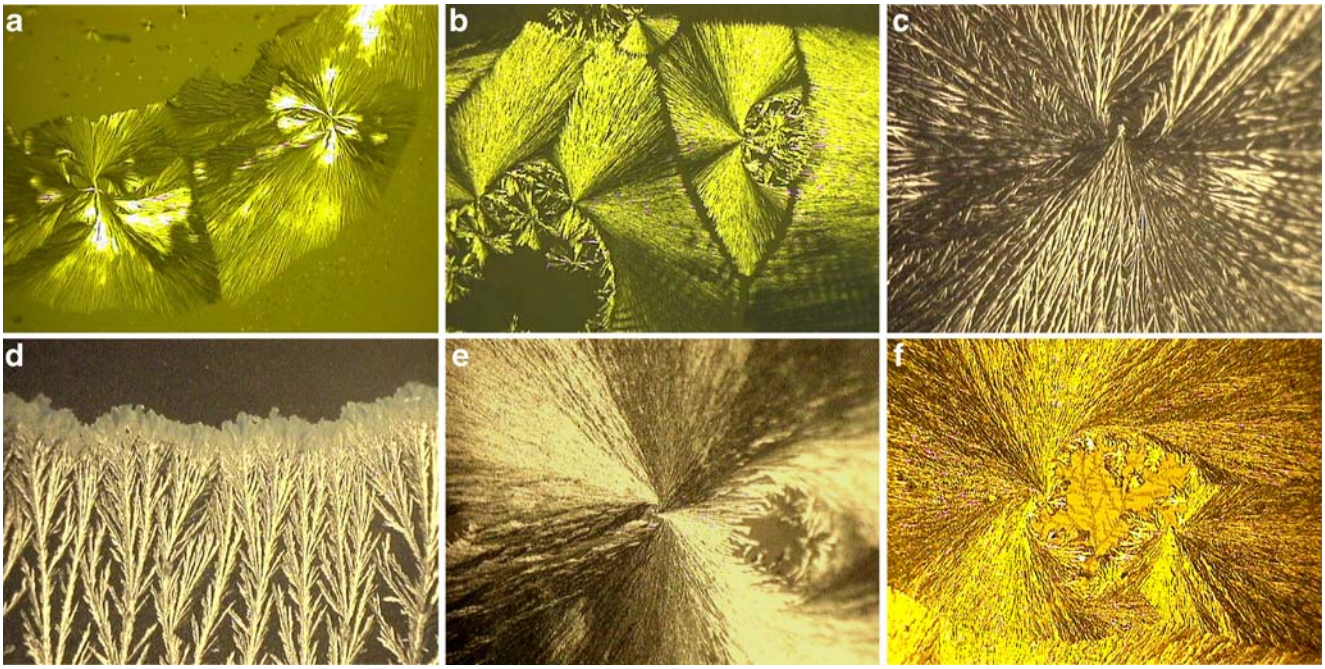


**Fig. 5** Typical polarizing microscopic dissipative patterns of NaPMA on a cover glass (**a**, **b**), a watch glass (**c**, **d**), and a glass dish (**e**, **f**). **a** 0.0006 monoM, **b** 0.02 monoM, **c** and **d** 0.00333 monoM, **e** and **f** 0.02 monoM; lengths of the picture frame are 1.0 mm and 1.4 mm (**a**) and 2.6×3.4 mm (**b**–**f**)

Microscopic pictures of NaPMA at 0.02 monoM of the initial polymer concentration are shown in Fig. 4, where full scales are 200 μm and 25 μm from a to f and g to l, respectively. These pictures support that the typical spherulites are formed whole areas of the dried film when the initial polymer concentration is high. However, small size of the hedrite crystals was often observed at the inner area from the broad rings, when the polymer concentrations were between 0.002 monoM and 0.01 monoM, though the pictures showing these were omitted in this work. When the initial polymer concentrations were lower than 0.0002 monoM, only the small hedrites were formed and the spherulites were not recognized from microscopic pictures.

Pictures a and b of Fig. 5 show the typical pictures of the polarizing microscopy of NaPMA around the broad ring area at 0.0006 monoM and 0.02 monoM of the initial polymer concentrations on a cover glass, respectively. The maltese cross patterns are observed for both pictures and support the formation of spherulite crystals. However, the crystals especially at 0.0006 monoM in Fig. 5a are highly distorted


**Fig. 6** Drying dissipative patterns of aqueous NaPMA solutions in a watch glass at 24 °C; 4 ml, after 54 h 25 m, **a** 0.000333 monoM, **b** 0.001 monoM, **c** 0.00333 monoM, **d** 0.01 monoM, and **e** 0.02 monoM

from the typical spherulite, which will be due to the collision and/or overlapping of the spherulite and also due to the hedrite structural formation at the low polymer concentration. Even at the high polymer concentrations, distortion of the spherulite is clear as is shown in Fig. 5b. Here, the hedrite crystals are segregated in a small area from the major spherulites.

## Macroscopic and microscopic drying patterns of NaPMA solutions in a watch glass

Figure 6 shows the typical macroscopic patterns of NaPMA solutions from 0.000333 monoM (a) to 0.02 monoM (e) in a watch glass. Several findings are clear. Firstly, the broad rings were observed for all the samples, and their sizes increased as polymer concentration increased (see also the crosses in Fig. 2). Secondary, the spherulites were formed especially at high polymer concentrations, and arrayed symmetrically and circularly. Thirdly, the single crystals were cut clearly at the outside edge of the broad and/or fine rings, which is clearly due to the coupling of the spherulite- and the broad ring-formation processes. The broad rings are formed by the convectional flow of the polymers accompanied with the water convection in the stages before the solidification. It should be mentioned here that the valleys

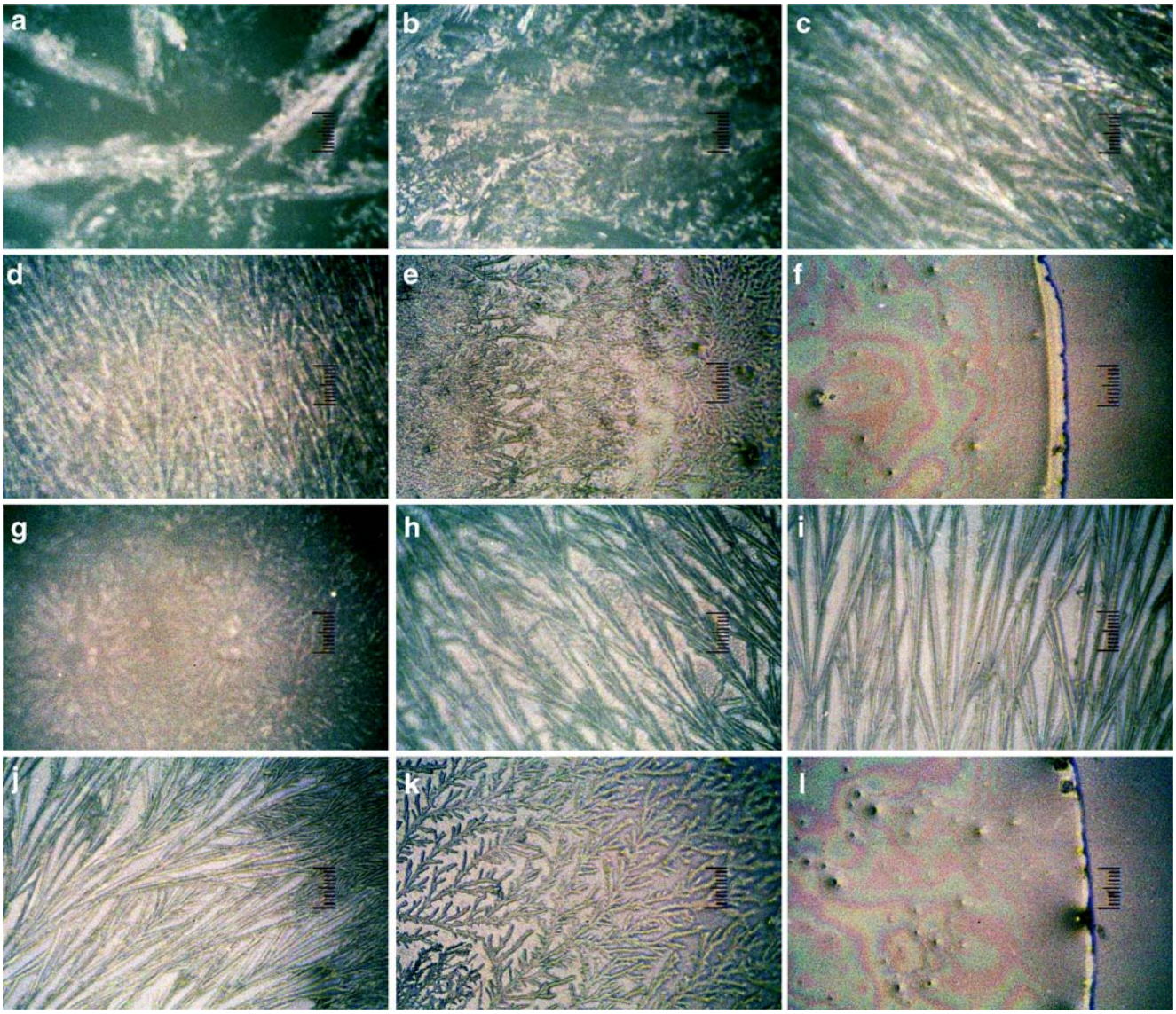


**Fig. 7** **a** Microscopic drying dissipative patterns of aqueous NaPMA solution in a watch glass at 24 °C. [NaPMA]=0.02 monoM (**a**–**f**) and 0.00333 monoM (**g**–**l**), pH=10.5, **a** to **f** and **g** to **l** are the pictures from center to the right edge, full scale is 100 μm. **b** Microscopic drying dissipative patterns of aqueous NaPMA solution in a watch glass at 24 °C. [NaPMA]=0.001 monoM (**a**–**f**) and 0.000333 monoM (**g**–**l**), **a** to **f** and **g** to **l** are the pictures from center to the right edge, full scale is 100 μm

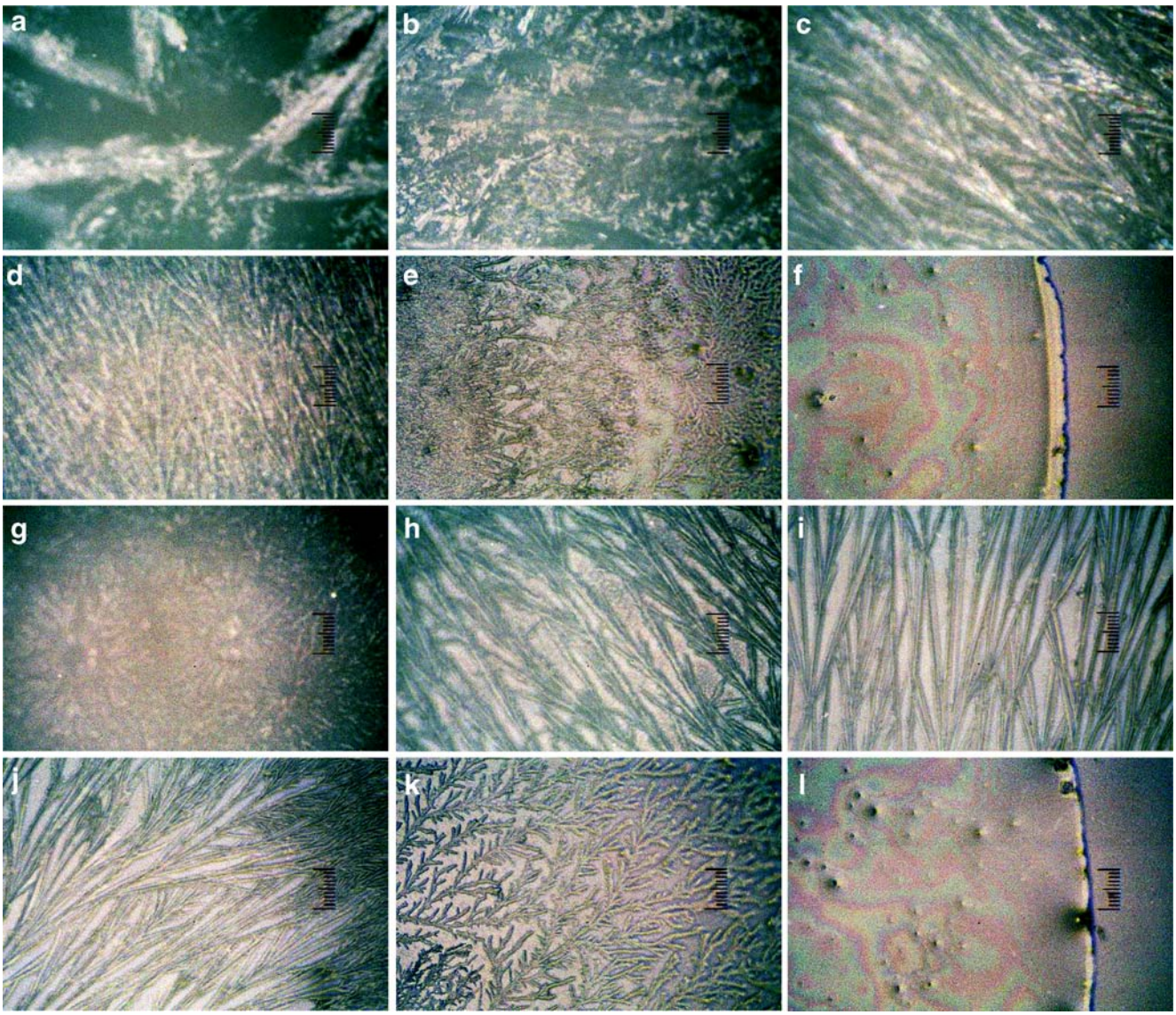


**Fig. 7** (continued)

of the spherulites especially inner area of the broad ring were quite deep and sharp (see Fig. 6e, for example).

The typical microscopic pictures were compiled in Fig. 7a and b. Polymer concentrations were 0.02 monoM (a–f of Fig. 7a), 0.00333 monoM (g–l of Fig. 7a), 0.001 monoM (a–f of Fig. 7b), and 0.000333 monoM (g–l of Fig. 7b), respectively. Length of the full scales inserted in the pictures is 100 μm. At 0.02 monoM and 0.00333 monoM, most crystals were spherulites. Interestingly, at the outside area along the outside edge of the broad ring, the hedrite crystals were apt to be formed. This will be due to the strong shearing forces by the convectional flow during solidification. As is clear in the pictures in Fig. 7b, the hedrite structures were formed rather than the spherulites at the low polymer concentrations of 0.001 monoM and 0.000333 monoM. These polymer concentration dependen-

**Fig. 8** Drying dissipative patterns of aqueous NaPMA solutions in a glass dish at 24 °C; 0.02 monoM, 4 ml, after 54 h 25 m

cies of the crystal structures are quite similar to those of poly(ethylene glycol) [52]. The polarizing microscopic pictures of NaPMA at 0.00333 monoM in a watch glass are shown in Fig. 5c and d. Fine structures of the fibrils of the spherulite are clearly seen in the pictures. The maltese crosses are seen in c and the coupling between the crystallization and the broad ring formation is clear in d, respectively. It should be noted here that the patterns of maltese cross in a watch glass shown in Fig. 5c was symmetrical and hedrite crystals were not observed. These support that the distortional forces by the convectional flow were not raised during the course of solidification in a watch glass and the segregation of the hedrite crystals did not take place.

## Macroscopic and microscopic drying patterns of NaPMA solutions in a glass dish

The macroscopic drying patterns of aqueous solutions of NaPMA at 0.02 monoM are shown in Fig. 8. Broad ring was observed at the outside area of the circular pattern in the central region. Size of the broad ring in a glass dish also decreased as polymer concentration decreased as is shown by crosses in Fig. 2. It should be noted here that the broad rings in a glass dish were rather broad compared with those on a cover glass and/or a watch glass. These observations support that the global convectional flow of the solvent water and the polymer solutes in a glass dish are not so regular and strong compared with those on a cover glass

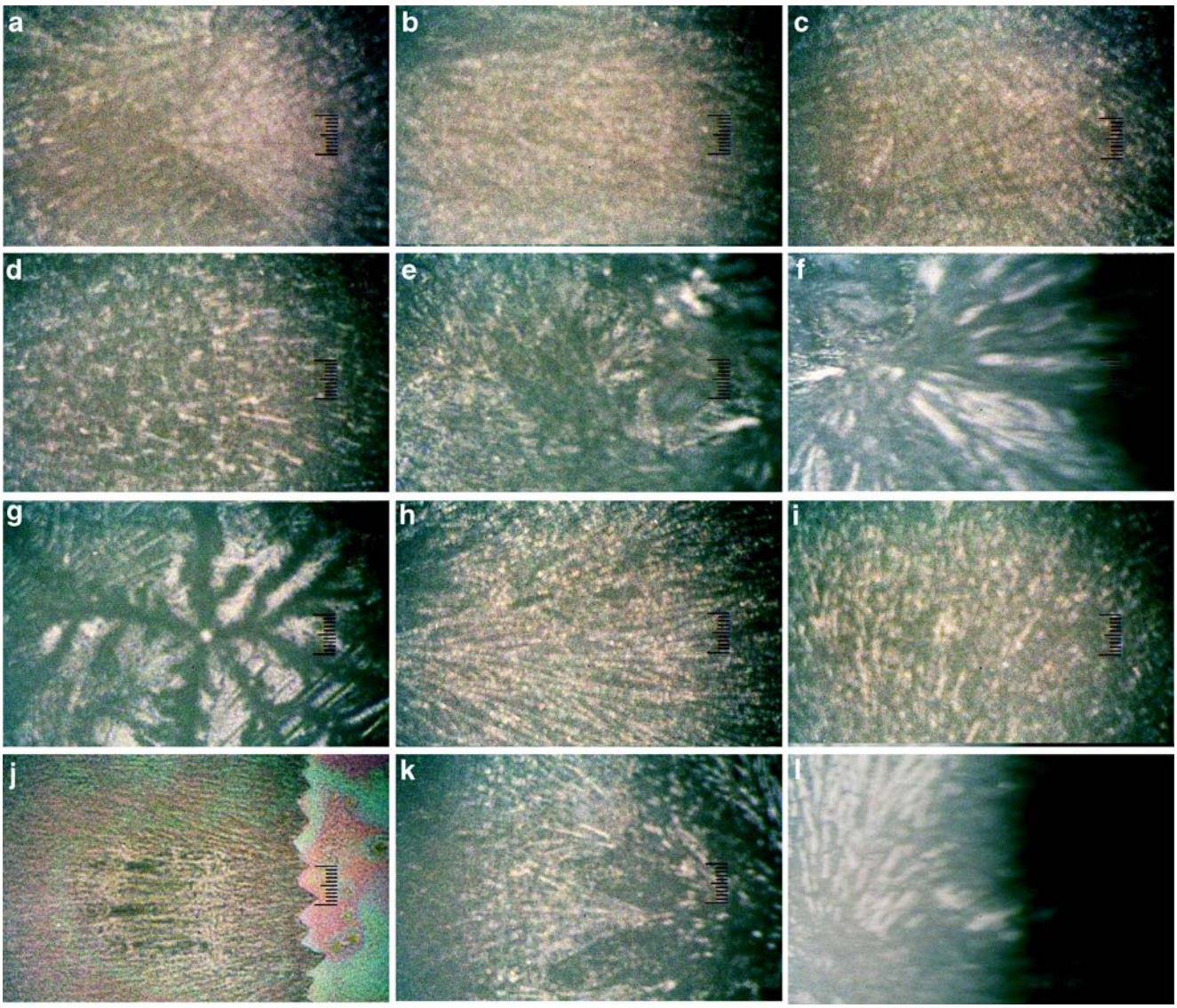


**Fig. 9** **a** Microscopic drying dissipative patterns of aqueous NaPMA solution in a glass dish at 24 °C. [NaPMA]=0.02 monoM (**a**–**f**), and 0.01 monoM (**g**–**l**), 5 ml, after 106 h 40 m, **a** to **f** and **g** to **l** are the pictures from center to the right edge, full scale is 100 μm. **b** Microscopic drying dissipative patterns of aqueous NaPMA solution in a glass dish at 24 °C. [NaPMA]=0.00375 monoM (**a**–**f**), and 0.00125 monoM (**g**–**l**), 5 ml, after 106 h 40 m, **a** to **f** and **g** to **l** are the pictures from center to the right edge, full scale is 100 μm

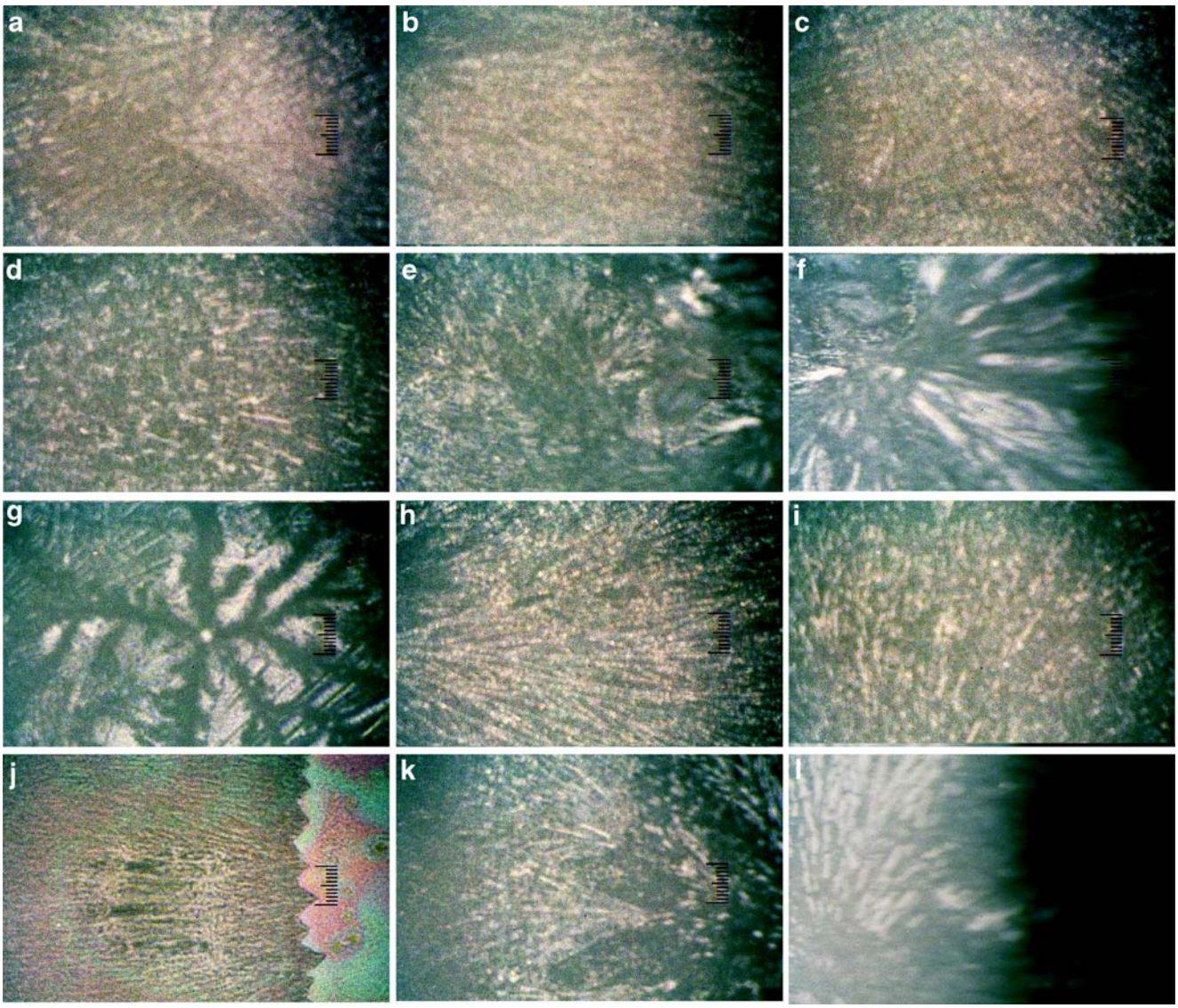


**Fig. 9** (continued)

and/or a watch glass. Furthermore, the difference in the directions of the drying frontiers between outward from center to outside in a glass dish and inward from outside to the center, will be one of the important factors for the broadness.

Figure 9a and b show the typical microscopic patterns of NaPMA at 0.02 monoM, 0.01 monoM, 0.00375 monoM, and 0.00125 monoM. When the polymer concentrations are high, the spherulite crystalline structures formed especially at the outside area. However, at the low polymer concentrations, spherulite crystallization was rather difficult, and the hedrites were formed instead. These observations in a glass dish are quite similar to those on a cover glass and a watch glass. The typical polarized microscopic pictures of NaPMA at 0.02 monoM in a glass dish are shown in Fig. 5e and f. The maltese cross patterns are observed in both pictures and again support the formation of spherulite crystals. Distortion of the spherulites is clearly shown in these pictures. Here, the hedrite crystals are segregated in a small area from the major spherulites. These observations in a glass dish are quite similar to those on a cover glass.

## Concluding remarks

In this work, drying dissipative patterns of aqueous solutions of sodium polymethacrylate, NaPMA were studied on a cover glass, a watch glass and a glass dish on macroscopic and microscopic scales. Several important results were obtained. Firstly, the spherulite and hedrite crystals were observed in the drying patterns of NaPMA, for the first time, in this work. The crystalline structures of

the dried film changed from hedrites to spherulites as NaPMA concentration increased. Secondary, the coupled patterns of the spherulites and the broad rings were formed irrespective of the substrates used, whereas the coupled patterns between the spherulites and the lamellaes, which were observed clearly for poly(ethylene glycol) in a watch glass, were not observed clearly for NaPMA. Formation of the coupled patterns supports the important role of the gravitational and Marangoni convections during the course of dryness. Thirdly, the broad ring size increased sharply as polymer concentration increased.

**Acknowledgments** Professor Emeritus Keisuke Kaji of Kyoto University is highly acknowledged for his valuable comments for this work. Financial supports from the Ministry of Education, Culture, Sports, Science, and Technology, Japan and Japan Society for the Promotion of Science are greatly acknowledged for Grants-in-Aid for Exploratory Research (17655046 to T.O.) and Scientific Research (B) (18350057 to T.O. and 19350110 to A.T.). Research fund from Rex Co. Tokyo to T.O. is also highly thanked.

## References

1. Okubo T (2006) Molecular and colloidal electro-optics. In: Stoylov SP, Stoimenova MV (eds), 573, Taylor & Francis
2. Okubo T (2008) In: Nagarajan R, Hatton TA (eds) Nanoparticles: syntheses, stabilization, passivation and functionalization. ACS, Washington DC, p 256
3. Gribbin G (1999) Almost everyone's guide to science. The universe, life and everything. Yale University Press, New Haven
4. Ball P (1999) The self-made tapestry pattern formation in nature. Oxford University Press, Oxford
5. Okubo T (2001) Beautiful world of colloids and interfaces (Japanese). Matsuo, Gifu
6. Terada T, Yamamoto R, Watanabe T (1934) Sci Paper Inst Phys Chem Res Jpn 27:173; Proc Imper Acad Tokyo 10:10
7. Terada T, Yamamoto R, Watanabe T (1934) Sci Paper Inst Phys Chem Res Jpn 27:75
8. Terada T, Yamamoto R (1935) Proc Imper Acad Tokyo 11:214
9. Nakaya U (1947) Memoirs of Torahiko Terada (Japanese). Kobunsya, Tokyo
10. Okubo T, Kimura H, Kimura T, Hayakawa F, Shibata T, Kimura K (2005) Colloid Polym Sci 283:1
11. Okubo T (2006) Colloid Polym Sci 285:225
12. Okubo T (2009) Colloid Polym Sci 287:167
13. Okubo T, Okamoto J, Tsuchida A (2009) Colloid Polym Sci 287:351
14. Okubo T, Okamoto J, Tsuchida A Colloid Polym Sci (2009). [doi:10.1007/s00396-009-2021-4]
15. Okubo T, Okamoto J, Tsuchida A (2008) Colloid Polym Sci 286:1123
16. Okubo T (2008) Colloid Polym Sci 286:1307
17. Okubo T (2006) Colloid Polym Sci 284:1191
18. Okubo T (2006) Colloid Polym Sci 284:1395
19. Okubo T, Okamoto J, Tsuchida A (2007) Colloid Polym Sci 285:967
20. Okubo T (2007) Colloid Polym Sci 285:1495
21. Okubo T, Okamoto J, Tsuchida A (2008) Colloid Polym Sci 286:385
22. Okubo T, Okamoto J, Tsuchida A (2008) Colloid Polym Sci 286:941
23. Yamaguchi T, Kimura K, Tsuchida A, Okubo T, Matsumoto M (2005) Colloid Polym Sci 283:1123
24. Okubo T (2006) Colloid Polym Sci 285:331
25. Vanderhoff JW (1973) J Polym Sci Symp 41:155
26. Nicolis G, Prigogine I (1977) Self-organization in non-equilibrium systems. Wiley, New York
27. Ohara PC, Heath JR, Gelbart WM (1997) Angew Chem 109:1120
28. Maenosono S, Dushkin CD, Saita S, Yamaguchi Y (1999) Langmuir 15:957
29. Nikoobakht B, Wang ZL, El-Sayed MA (2000) J Phys Chem 104:8635
30. Ung T, Litz-Marzan LM, Mulvaney P (2001) J Phys Chem B 105:3441
31. Okubo T, Onoshima D, Tsuchida A (2007) 285:999
32. Okubo T, Kanayama S, Ogawa H, Hibino M, Kimura K (2004) Colloid Polym Sci 282:230
33. Shimomura M, Sawadaishi T (2001) Curr Opin Coll Interf Sci 6:11
34. Okubo T, Yamada T, Kimura K, Tsuchida A (2006) Colloid Polym Sci 284:396
35. Kimura K, Kanayama S, Tsuchida A, Okubo T (2005) Colloid Polym Sci 283:898
36. Okubo T, Shinoda C, Kimura K, Tsuchida A (2005) Langmuir 21:9889
37. Okubo T, Kanayama S, Kimura K (2004) Colloid Polym Sci 282:486
38. Okubo T, Itoh E, Tsuchida A, Kokufuta E (2006) Colloid Polym Sci 285:339
39. Okubo T, Yokota N, Tsuchida A (2007) Colloid Polym Sci 285:1257
40. Deegan RD, Bakajin O, Dupont TF, Huber G, Nagel SR, Witten TA (1997) Nature 389:827
41. Deegan RD, Bakajin O, Dupont TF, Huber G, Nagel SR, Witten TA (2000) Phys Rev E 62:756
42. Cachile M, Benichou O, Cazabat AM (2002) Langmuir 18:7985
43. Cachile M, Benichou O, Poulard C, Cazabat AM (2002) Langmuir 18:8070
44. Palmer HJ (1976) J Fluid Mech 75:487
45. Anderson DM, Davis SH (1995) Phys Fluids 7:248
46. Pouth AF, Russel WB (1998) AIChEJ 44:2088
47. Burelbach JP, Bankoff SG (1998) J Fluid Mech 195:463
48. Matar K, Craster RV (2001) Phys Fluids 13:1869
49. Hu H, Larson RG (2002) J Phys Chem B 106:1334
50. Rabani E, Reichman DR, Geissler PL, Brus LE (2003) Nature 426:271
51. Fischer BJ (2002) Langmuir 18:60
52. Okubo T, Okamoto J, Takahashi S, Tsuchida A (2009) Colloid Polymer Sci. doi:10.1007/s00396-009-2049-5